iTrack: Tracking Indicator LEDs on APs to Bootstrap mmWave Beam Acquisition and Steering

Muhammad Kumail Haider and Edward W. Knightly
Rice University, Houston TX
{kumail.haider,knightly}@rice.edu

ABSTRACT

We present iTrack, a system which steers mmWave beams at mobile devices by tracking the indicator LEDs on wireless APs to passively acquire direction estimates, and demonstrate that iTrack acquires and maintains beam alignment at the narrowest beamwidth level even in case of device mobility, without incurring any training overhead. Our implementation on custom dual-band hardware testbed shows that iTrack acquires direction estimates within 4.5 degrees of the ground truth and achieves beam steering accuracy of more than 97% while in tracking mode, without incurring any in-band training or feedback.

ACM Reference Format:
Muhammad Kumail Haider and Edward W. Knightly. 2018. iTrack: Tracking Indicator LEDs on APs to Bootstrap mmWave Beam Acquisition and Steering. In *Proceedings of 19th International Workshop on Mobile Computing Systems and Applications (HotMobile'18).* ACM, New York, NY, USA, 6 pages. https://doi.org/10.1145/3177102.3177105

1 INTRODUCTION

The ever-increasing demand for high speed wireless connectivity to support applications like virtual and augmented reality, uncompressed video streaming and wireless docking is straining the capacity of current WiFi and cellular networks [1]. The wide GHz-scale bandwidth coupled with phased array antennas to realize high directionality in the mmWave spectrum, spanning a wide range of frequencies from 30 GHz to 300 GHz and beyond, can solve this problem by realizing data rates of up to 100 Gb/sec [8]. However, a key challenge in exploiting this expansive bandwidth and high data rates is that end nodes need to align their beams to establish a highly directional link, before any communication can happen.

To this end, existing commercial products [14, 19] and WLAN standards like 802.11ad [11] and 802.11ay [8] employ beam-search based training mechanisms, where one node sends training frames across all its beams while the other uses pseudo-omni antenna patterns to identify the strongest beam. Although this training, when repeated at both ends, discovers the strongest pair of beams with maximum data rates, the process may take 10's of *ms*. This overhead represents missed opportunity to transmit 100's of Mb, severely degrading throughput and disrupting high-rate, low-latency applications. Moreover, the overhead worsens for multi-user transmissions [5, 8] and in Next-Gen THz networks with no pseudo-omni reception [10], increasing the order of beam-search space from $2N$ to N^2 for N beams at either end. Mobile nodes present an even greater challenge, where beam alignment may be repeatedly lost due to mobility, requiring more training epochs and incurring overhead each time.

We present iTrack, a system which steers mmWave beams at mobile devices by tracking indicator LEDs on wireless Access Points (APs) to passively acquire direction estimates, eliminating the need for beam search at the clients. Our design is motivated by the observation that most off-the-shelf wireless APs are equipped with light sources like notification LEDs, which are in close proximity to their phased array antennas. Therefore, by tracking this indicator LED at client devices using off-the-shelf light sensors (e.g., photodiodes), we can "point" the client's antenna beams towards the AP, without requiring any in-band training or beam search.

We demonstrate that iTrack acquires and maintains beam alignment at the narrowest beamwidth level at the clients even in case of device mobility, without incurring any training overhead. Moreover, our design is scalable with the number of clients, such that the AP can simultaneously align beams with multiple clients by performing a beam sweep only once at its end; client beams are selected via out-of-band light sensing.

For this, we exploit the pseudo-optical properties of mmWave channels; specifically the dominant Line of Sight (LOS) propagation, limited scattering and reduced multipath due to very short wavelength [2, 6]. Since visible light band exhibits similar dominant LOS propagation [3], our key idea is to estimate the Angle of Arrival (AOA) corresponding to the LOS path from the AP's indicator LED, and approximate it as the AOA in the mmWave band due to close proximity of AP's LED and its phased array antenna. Therefore, we select the client-side beam as the one with the highest gain along the AOA for the LOS path. We show that by passively tracking AP's indicator LED, an iTrack client continuously adapts its antenna beams without requiring any beam training.

The key challenge in exploiting the light source at the AP for this direction tracking is that, unlike lasers, light intensity from LEDs (or common light bulbs) is *incoherent*, and off-the-shelf light sensors can only measure the *intensity* of the incident light. Therefore, AOA estimation techniques in radio bands via antenna array phase difference (e.g., [21]) cannot be used. For this, we devise a novel method for incoherent-light Angle of Arrival (il-AOA) estimation by using an array of light sensors. Our key technique is to approximate the ratio of light intensities at adjacent sensors as a function of their AOA only by exploiting their angular separation on the

HotMobile'18, February 12–13, 2018, Tempe, AZ, USA

ACM ISBN 978-1-4503-5630-5/18/02…$15.00
https://doi.org/10.1145/3177102.3177105

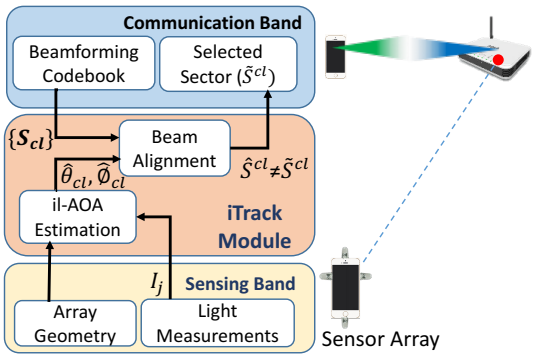

Figure 1: iTrack node architecture.

array. We then estimate the AOA of the LOS path without requiring any calibration or knowledge of the AP's position or client's orientation. Moreover, our method estimates il-AOA in both azimuth and elevation planes, allowing us to steer beams for both 2-D and 3-D beamforming codebooks.

We implement iTrack on a dual-band hardware platform and perform rigorous experiments to evaluate the key components of iTrack design. Our preliminary results are promising; showing that iTrack estimates il-AOA to within 4.5° without any knowledge of the AP or client's position. Moreover, in various rotational mobility scenarios, iTrack can steer beams correctly more than 97% of instances, without incurring any in-band training overhead or feedback. In the future, we plan to extend the experimental setup to include our wide-band platform with phased array antennas [14] and THz transceivers [10].

2 ITRACK DESIGN

In this section, we first present iTrack's system architecture. We then describe the beam alignment protocol and our novel method to estimate the il-AOA using light measurements from the AP's indicator LED.

2.1 System Architecture

The iTrack architecture is divided into two distinct bands; a *Communication Band* and a *Sensing Band*. The former comprises of mmWave band radios and phased array antennas at the AP and client nodes, over which data communication takes place. In most modern systems, the phases of antenna elements are defined via a 3-D beamforming codebook ($\{\mathbf{S}\}$), such that by switching between codebook entries, beams can be electronically steered, discretizing the space around the array into virtual "sectors" [2]. While our design is compatible with any directional antenna design, for the rest of this section we assume phased array antenna system for both AP and clients. The Sensing Band comprises of an indicator LED at the AP and multiple light sensors at the client. We require that this LED be distinguishable from ambient light, which can be achieved by using RGB photodiodes for colored LEDs on the AP or by using recent solutions (e.g., [24]) to distinguish light sources. In any case, we do not require any data communication or signaling in the Sensing Band.

Fig. 1 depicts iTrack client node architecture. The client equips an array of J light sensors to measure light intensity (I) from the AP's LED. The set of intensities $\{I\} = I_j, j = 1, .., J$ is input to the iTrack software module (shown by the middle block), which has two main components: *(i) il-AOA Estimation Block* which uses light measurements to estimate the azimuth and elevation components $(\hat{\theta}_{cl}, \hat{\phi}_{cl})$ of the il-AOA (Sec. 2.3); and *(ii) Beam Alignment Block* which estimates client's highest strength sector $\hat{S}_{cl}$ using the il-AOA estimates (Sec. 2.2). This estimated sector is then passed on to the Communication Band, and is used as the "selected sector" $(\tilde{S}_{cl})$ for directional transmission and reception.

2.2 Beam Alignment Protocol

Design Principle: Due to extremely small wavelength, mmWave channels are shown to have limited scattering, which is usually characterized using geometric channel models as follows [2, 6]:

$$\mathbf{H} = C \sum_{l=1}^{L} \alpha_l \, \mathbf{a}_T(\theta_{T,l}\,,\, \phi_{T,l}) \; \mathbf{a}_R(\theta_{R,l}, \phi_{R,l}), \tag{1}$$

where C is a normalization constant, L is the number of physical paths, α_l is the path gain, $\mathbf{a}_T$ and $\mathbf{a}_R$ are the array response vectors at the transmitter and the receiver, and θ and ϕ denote the azimuth and elevation components of the corresponding Angle of Departure (AOD)/AOA respectively[1]. Due to dominant LOS propagation of mmWave channels shown in prior measurement studies and channel models [1, 22], we expect the LOS channel component to have the maximum gain. Therefore, our key idea is to exploit the AP's LED to estimate the il-AOA $(\hat{\theta}_{cl}, \hat{\phi}_{cl})$ of the LOS path at the client using light measurements only, and then select the client-side beam with maximum directivity gain (using known beam patterns) along the estimated AOA. As such, we avoid any mmWave in-band training or beam-search at the client. Note that we use the term il-AOA to specify the AOA of the physical LOS path between the AP and the client measured using light intensities. In particular, we use the client's codebook $\{\mathbf{S_{cl}}\}$ to find the beam (or sector for discretized codebooks) $\hat{S}_{cl}$ which has maximum gain along $(\hat{\theta}_{cl}, \hat{\phi}_{cl})$, as follows:

$$\hat{S}_{cl} = \arg \min_{S_{cl,m}; m=1\ldots N} \left| \angle\,(\Theta_{S_{cl,m}}, \Phi_{S_{cl,m}}) - (\hat{\theta}_{cl}, \hat{\phi}_{cl}) \right| \tag{2}$$

where $(\Theta_{S_{cl,m}}, \Phi_{S_{cl,m}})$ are the central azimuth and elevation angles of any client sector $S_{cl,m}$.

Using this estimation framework, we design iTrack to comprise of the following two phases.

Beam Acquisition: This is the initial phase where maximal strength sectors are not known at the AP or the clients e.g., at association or after link breakage. During this phase, an iTrack client estimates its maximal strength sector using light measurements as described above, and uses this sector to receive in mmWave band while the AP does a beam sweep at its end. The client then gives a feedback about AP's maximal strength sector to the AP. This may be followed by an optional beam refinement phase, as defined in 802.11ad [11], where the client can use the il-AOA estimate to do a local search in the neighboring sectors to refine beam selection. In any case, an exhaustive search is not required at the client end if il-AOA estimates are available.

In case of multi-user training, the AP can simultaneously train with any number of clients by doing a single beam sweep and getting feedback from the clients. As such, if the AP has N_{AP} sectors and trains with M clients, each with $N_{cl,m}$ sectors, then iTrack

[1]Due to channel reciprocity, only the AOA or the AOD needs to be estimated.

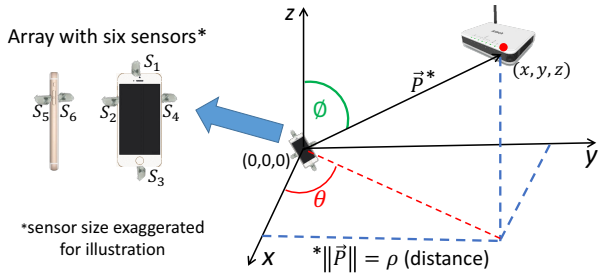

Figure 2: Indicator-LED sensing via client's sensor array.

requires beam search only over N_{AP} sectors during beam acquisition, compared to $N_{AP} \cdot \sum_{m=1}^{M} N_{cl,m}$ sector combinations in case of 802.11ad based pseudo-omni training or $(N_{AP})^M \cdot \prod_{m=1}^{M} N_{cl,m}$ in case of the optimal exhaustive search based training.

Beam Steering: After a directional link is established via Beam Acquisition, iTrack enters the Beam Steering phase, where it passively tracks the il-AOA from the AP's LED and continuously estimates the best client-side sector $\hat{S}_{cl}$ using the il-AOA estimates. Due to client mobility, if this best sector estimate becomes different from the selected sector $\tilde{S}_{cl}$ being used for communication, an interrupt $(\tilde{S}_{cl} \leftarrow \hat{S}_{cl})$ is passed to the MAC layer to adapt the current sector $\tilde{S}_{cl}$. As such, iTrack steers client-side beams without incurring any training or feedback overhead.

Moreover, the AP is oblivious to any changes in client-side sectors, making beam steering completely distributed. However, if beam alignment is lost due to unavailability of light estimates (e.g., due to self-blockage) or AP's sectors require adaptation, iTrack enters Beam Acquisition again.

2.3 il-AOA Estimation

Here we describe the visible light channel model and our method to estimate both azimuth and elevation components of the il-AOA for the LOS path using light measurements only.

Visible Light Channel Model: The intensity (I) of light received at a sensor is modeled by the Lambertian radiation pattern for LOS propagation [3] as follows:

$$I(\rho, \gamma, \psi) = T \cdot A \cdot g(\psi) \cdot \left(\frac{m+1}{2\pi}\right) \cdot cos^m(\psi) \cdot \frac{cos(\gamma)}{\rho^2} \tag{3}$$

where T is the transmit power, A is sensor area, γ is the irradiance angle between the vector from light source to sensor and the normal vector to the source, ρ is the source-sensor distance and ψ is the AOA at the *sensor*. g is optical concentrator, which is a constant if ψ lies within the field-of-view of the sensor. m is the Lambertian order, which is 1 for common indoor LEDs. It follows that the light intensity varies inversely to distance, AOA and irradiance angle.

Problem Formulation: Fig. 2 depicts an AP at position (x, y, z) with respect to an iTrack client, where the reference frame is centered at the client's planar phased array, with *z-axis* orthogonal to the array. By geometry, angles θ_{cl} and ϕ_{cl} shown in the figure correspond to the azimuth and elevation components of the AOA from the AP to the client's array for the LOS path. Our objective is to estimate $(\hat{\theta}_{cl}, \hat{\phi}_{cl})$ as the il-AOA using the incoherent light from the AP's LED using off-the-shelf light sensors.

Sensor Array Design: The two components of the il-AOA cannot be estimated using a single sensor since the light intensity depends on both the position of and the AOA at the sensor. Moreover, since the sensor may have an arbitrary orientation, the AOA (ψ) at the sensor may not be the same as the il-AOA, but a projection of it along the sensor's axis. Our key technique is to exploit an array of multiple sensors with known angular separation to estimate θ_{cl} and ϕ_{cl}. When introducing more sensors, the entropy of measurements is maximized by placing sensors at right angles, since it gives maximum angular separation. Therefore, in our sensor array design, we use at least six sensors arranged mutually orthogonally on the six facets of a mobile device. For the rest of this section, we discuss this case of six-sensor array, but the formulation can easily be extended to larger array sizes.

Estimation Method: Fig. 2 depicts an iTrack client with $J = 6$ light sensors arranged mutually orthogonally. In this case, the light intensity from the AP's LED received at the j^{th} sensor of the client is given as:

$$I_j = C \cdot cos(\psi_j) \cdot \frac{cos(\gamma_j)}{(\rho_j)^2} \tag{4}$$

where C is a constant parameter for sensors of same type, and ρ_j is the distance between the LED and the j^{th} sensor. If $\overrightarrow{P} = [x, y, z]^T$ is the position vector to the AP's LED and $\overrightarrow{P_j}$ is that of the j^{th} sensor (with unit normal vector $\overrightarrow{u_j}$), then angles γ_j and ψ_j can be computed as:

$$cos(\gamma_j) = \frac{\overrightarrow{z} \odot (\overrightarrow{P_j} - \overrightarrow{P})}{\rho_j} \tag{5}$$

$$cos(\psi_j) = \frac{\overrightarrow{u_j} \odot (\overrightarrow{P} - \overrightarrow{P_j})}{\rho_j} \tag{6}$$

Since the size of mobile devices is usually much smaller compared to the AP-client distance, our key technique is to approximate the irradiance angle and distance from the AP to be the same at all sensors ($\forall j, \gamma_j = \gamma, \rho_j = \rho$). With this approximation, the ratio of intensities at any two adjacent sensors is a function of their AOA only, independent of ρ and γ:

$$\frac{I_{j1}}{I_{j2}} \approx \frac{cos(\psi_{j1})}{cos(\psi_{j2})} \tag{7}$$

Since the arrangement of sensors is fixed and known at the client, we consider the ratio of intensities at adjacent sensors in three perpendicular planes to estimate the il-AOA component in that plane, without requiring client's position or orientation. For example, in the case when sensors are arranged mutually orthogonally, this difference in AOA is in fact 90°, such that we can make the substitution $cos(\psi_{j2}) = sin(90 - \psi_{j1}))$ in Eq.7 to estimate ψ_{j1} as follows:

$$\hat{\psi}_{j1} = tan^{-1}\left(\frac{I_{j2}}{I_{j1}}\right) \tag{8}$$

Note that it is not necessary that light sensor array and client's phased array are coplanar and aligned; only the mapping is required such that angles estimated using the light-sensor array can be rotated to find angles with respect to the mmWave phased array. However, for simplicity and without loss of generality, here we assume that the two arrays are aligned, so that the same reference frame defined in Fig. 2 can be used for the light sensor array as

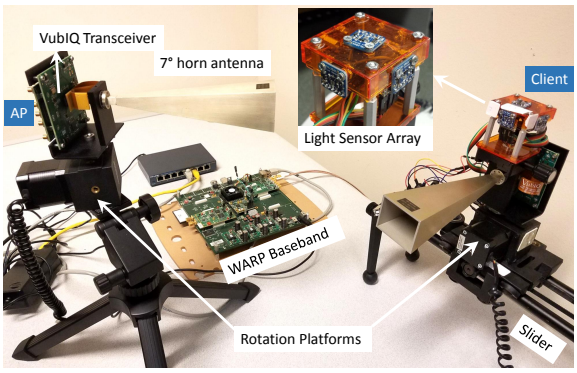

Figure 3: Dual-band hardware platform.

well. With this simplification, we can define $\overrightarrow{u_j}$ as unit vectors along +x,-x,+y,-y,+z,-z axes for the six mutually orthogonal sensors.

Moreover, by array geometry, at most three sensors on the array can have LOS path to the AP, one along each axis (I_x, I_y, I_z). Using the negligible array dimension approximation and solving for $cos(\psi_j)$ at adjacent sensors in the three perpendicular planes, we estimate θ_{cl} and ϕ_{cl} as follows:

$$\hat{\theta}_{cl} = tan^{-1}\left(\frac{I_y}{I_x}\right) \quad , \quad \hat{\phi}_{cl} = tan^{-1}\left(\frac{\sqrt{I_x^2 + I_y^2}}{I_z}\right) \tag{9}$$

3 IMPLEMENTATION AND EVALUATION

In this section, we first describe our implementation of iTrack on a custom dual-band hardware platform, and then discuss our preliminary experiments to evaluate key components of iTrack for indoor mmWave networks.

3.1 Dual-band Hardware Testbed

For our initial evaluation, we select 60 GHz transceivers for communication in the mmWave band, and develop a custom hardware testbed comprising of an AP and a client node, as depicted in Fig. 3. In particular, we develop programmable nodes using VubIQ transceiver system, operating in the 57-64 GHz unlicensed frequency band with 1.8 GHz bandwidth (compliant with 802.11ad) and WARP baseband (a software-defined radio platform). To achieve narrow sector widths, we use horn antennas with 7° beamwidth at both AP and client sides. To implement beam-steering and rotation, both nodes are mounted on Cine-Moco motion platform with a rotation precision of 0.01°. Using this platform, antennas are rotated in discrete steps to emulate discretized sectors (predefined by a codebook) to achieve sector sweeps and beam steering.

Further, we use an off-the-shelf Lumileds LED (1200 lm, 33V, 100° viewing angle) at the AP. For the client, we build a $7 \times 7 \times 3$ cm array (emulating dimensions of a big smartphone or a tablet) with six sensors (Adafruit TSL-2591, 180° FoV).

3.2 Experimental Setup

We evaluate the accuracy of il-AOA estimation and client-side sector selection for both phases in iTrack (i.e., Beam Acquisition and Beam Steering). For beam steering, our initial experiments encompass various rotational mobility scenario, whereas we leave evaluation of translational mobility for future version of this paper.

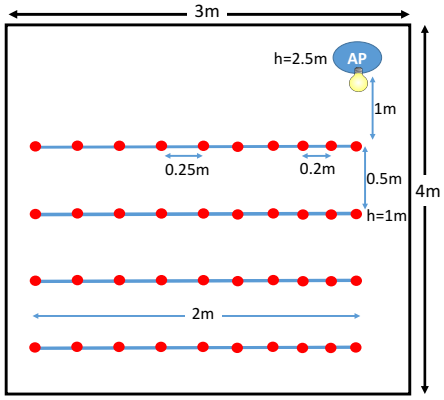

Figure 4: Testbed setup in the lab environment.

For this, we setup the dual-band testbed in a lab within $4 \times 3 \times 5$m space with the AP at 2.5m height in a corner. For the client, we consider 40 different locations along four rows at radial distances 1m, 1.5m, 2m and 2.5m respectively from the AP at 1m height, as shown in Fig. 4. This setup helps us evaluate iTrack performance under a broad set of AP-client distances and angular separations, which affect the light intensity measurements and beam steering. Further, at each client location, we rotate the client by 60° in steps of 1° and take measurements across both bands. As such, our experiments also encompass (61×40) different position-orientation combinations for evaluating beam acquisition accuracy in addition to rotation. Note that there is always a LOS path in the visible light and 60 GHz bands in these experiments; we leave evaluation of blockage scenario for future work.

3.3 Results

3.3.1 Beam Acquisition Phase. We first evaluate the accuracy of il-AOA estimation using light measurements. To identify various sources of estimation error, we also perform light channel model based simulations to analyze the performance of sensor arrays with various dimensions, and for comparison with our over-the-air experiments. Fig. 5a depicts the CDF of il-AOA estimation error. First, for simulation of an array of negligible dimensions (0.01cm), we observe an almost perfect il-AOA estimation accuracy, which validates our key technique. Second, simulation results for a 7cm array (same dimensions as our testbed array) show up to 2° estimation error, indicating that array dimension plays a key role in determining the accuracy of our method. Sensors can be placed close to device edges to further minimize this error and achieve better accuracy. However, for our tested, we develop a cubic shaped array with relatively large distance between sensors to test the viability of our method for arrays with relatively larger dimensions.

Next we analyze the performance in over-the-air experiments. The blue curve for measurement results indicates that the estimation error is within 4.5° of the true AOA even for our reasonably large cubic array. The error is also higher than the simulations due to the deviation of intensity measurements from the channel models, which we discover increases with distance between light source and sensors. To investigate this further, we compute the average il-AOA estimation error across all locations in the four rows of our setup, such that the average distance increases across the

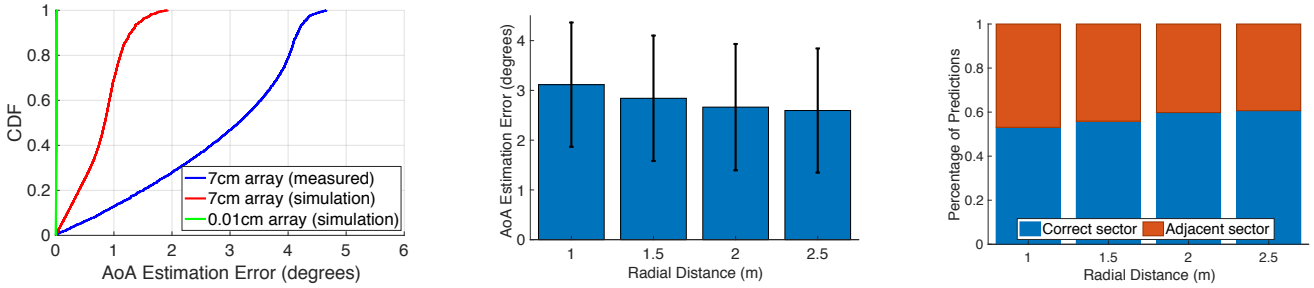

(a) CDF of il-AOA estimation error. **(b) il-AOA estimation vs. distance** **(c) Sector selection accuracy.**

Figure 5: Client-side sector selection during beam acquisition via il-AOA estimation using light measurements.

rows. Fig. 5b shows that as the radial distance of the rows increases (plotted along the *x-axis*), the average il-AOA estimation error in fact decreases. This is because of an additional factor which impacts our il-AOA estimation accuracy; the validity of our negligible array dimensions approximation, which improves with an increase in distance. Results show that this factor is dominant in determining the il-AOA estimation accuracy.

Finally, we evaluate sector selection accuracy at the client in our experiments, by comparing sectors selected by iTrack to the ground truth by geometry. Fig. 5c depicts the client-side sector selection accuracy, averaged across locations and orientations for each of the four rows, with the radial distance of rows plotted along the *x-axis*. We observe that for all instances, the correct client-side sector is selected more than 50% of times, with selection accuracy improving slightly with distance. This is consistent with the improving il-AOA estimation accuracy with increasing AP-client distance. Further, the selected sector differs from the true maximal strength sector at most by 1 sector for all location, orientation combinations.

Findings: Even with an array of reasonably large edge-dimensions, iTrack estimates il-AOA within 4.5° *of the ground truth. Higher accuracy can be realized by placing sensors close to device edges to further reduce inter-sensor distance, a key factor affecting the estimation accuracy. Further, iTrack acquires client beams to within 1 sector of the true highest strength sector in all cases without any in-band training. Thus our light based il-AOA estimation eliminates the need for exhaustive beam search at mobile clients.*

3.3.2 Beam Steering Phase. Next we evaluate the beam steering capability of iTrack for various rotational mobility scenario in the aforementioned experiments. A key factor that impacts iTrack's beam steering accuracy is the frequency at which il-AOA estimates are computed. This is determined by multiple factors, such as sampling frequency of light sensors and computational resources of smart devices. Moreover, rotational speed of the client may also affect steering accuracy; the faster the speed, the harder the tracking since the client may rotate more for the same estimation frequency. Therefore, instead of evaluating all these factors separately, we normalize the estimation frequency to client's rotation, such that an il-AOA estimate is computed for every δ degrees of client's rotation. Here we present results for four δ values: $1°, 2°, 5°$ and $10°$.

First we analyze rotation estimation accuracy by computing the change in estimated il-AOA between the initial and final orientations of the client. Fig. 6a plots the CDF of rotation estimation error for the four δ values. We observe that when il-AOA estimates

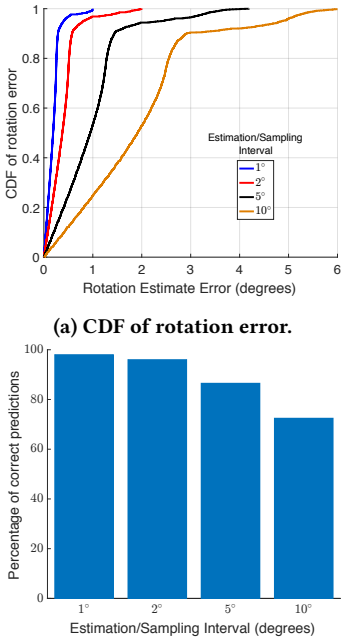

(a) CDF of rotation error.

(b) Beam steering accuracy.

Figure 6: Rotation with various estimation intervals.

are computed most frequently (every 1° of client rotation), the estimation error is the lowest since we have the most light measurements to estimate the same rotation compared to the other cases. Further, we observe that the rotation estimates are within 0.5° of the true value for more than 90% of instances, which is much higher than absolute il-AOA estimation accuracy in Fig. 5a. This is because il-AOA estimation is affected by the AP-client relative angle and distance, which predominantly determines the deviation of measured results from the theoretical channel models. However, for estimating rotation, this il-AOA estimation error has the same location bias, and this component of error is cancelled out when computing the change in il-AOA to find client rotation. Moreover, the graph also shows that as the estimation interval (δ) increases, rotation estimation error also becomes large, since there is a greater change in client's orientation between two measurements.

Next we analyze the client-side sector steering accuracy in Fig. 6b for various values of δ plotted along the *x-axis*. Consistent with a high rotation estimation accuracy, we observe that iTrack is able to steer client sectors to the true highest strength sectors for more

than 97% of the time with $\delta = 1^\circ$. Although steering accuracy decreases with an increase in estimation interval, even with a high interval of 10°, which represents very high rotational speeds or conversely very low sampling rate of sensors, iTrack computes the correct sectors more than 70% of the time.

Findings: By estimating changes in il-AOA from the AP's light source, iTrack is able to track rotation at even higher accuracy than it does absolute il-AOA, leading to almost 97% *steering accuracy when il-AOA estimates are computed at a modest rate of every* 1° *of client rotation. Consequently, once a mmWave link is established, iTrack can maintain alignment at the narrowest beamwidth level despite device mobility solely by passive light sensing.*

4 RELATED WORK

Visible Light Sensing: There are few existing works on AOA estimation using incoherent light. [9] uses model driven AOA calculation for localization from *multiple* light sources. In [24], non-linear intensity differences between two sensors of different fields of view was employed to estimate the AOA. However, it is limited to the azimuth plane due to 1-D AOA estimation and requires calibration of sensors.

mmWave Beam Training: *In-band* solutions to reduce training overhead include model-driven beam steering and channel profiling [20, 25], efficient beam searching [17, 23], sector switching and backup paths [7, 15, 18], and beamwidth adaptation [7]. These solutions help reduce steering overhead and maintain alignment in certain environments, however, they still incur training overhead when constructing channel profiles, searching for backup or redundant paths, or SNR degradation when switching to wider beams. In this work, we target to eliminate beam search at mobile devices by obtaining direction estimates from existing LEDs on APs. Nonetheless, prior solutions can be integrated to reduce training overhead for AP-side sweeps or when light measurements are not available.

Lastly, prior *out-of-band* solutions also address mobile clients in directional networks e.g., via session transfer to legacy bands [11, 16], AOA estimation in legacy bands to eliminate exhaustive search [12], and using sensors on mobile devices [4, 13, 23]. In contrast, we use passive light sensing which has much less power requirements than mechanical sensors, requires no communication in the sensing band, and is more resilient to multipath due to dominant LOS propagation of visible light.

5 CONCLUSION AND FUTURE WORK

In this paper, we present iTrack to steer mmWave beams at mobile devices by tracking the indicator LEDs on wireless APs to passively acquire direction estimates, and demonstrate that iTrack acquires and maintains beam alignment despite device mobility, without incurring any training overhead. We also implement our system on a custom dual-band platform for proof-of-concept. Our preliminary experiments show that iTrack estimates the incoherent-light AOA to within 4.5 degrees and steers beams correctly more than 97% of instances while in tracking mode, without incurring any in-band training or feedback.

Our next step is to extend the experimental setup to include our wide-band platform with phased array antennas [14] and THz transceivers [10], and using RGB photodiodes to track colored LEDs on commercial APs. We also plan to explore further interesting applications of our work, especially LOS path blockage and self blockage detection using light sensing. In such cases, even if AOA estimate is not available, some steering directions can be eliminated in the beam-search space when performing beam training.

6 ACKNOWLEDGEMENTS

This research was supported by Cisco, Intel, the Keck Foundation, and by NSF grants CNS-1642929 and CNS-1514285.

REFERENCES

[1] Abari, O., Hassanieh, H., Rodriguez, M., and Katabi, D. Millimeter Wave Communications: From Point-to-Point Links to Agile Network Connections. In *Proc. of ACM HotNets* (2016).
[2] Alkhateeb, A., El Ayach, O., Leus, G., and Heath, R. W. Channel Estimation and Hybrid Precoding for Millimeter Wave Cellular Systems. *IEEE JSTSP 8*, 5 (2014), 831–846.
[3] Barry, J. R. *Wireless Infrared Communications*, vol. 280. Springer Science & Business Media, 2012.
[4] Doff, A. W., Chandra, K., and Prasad, R. V. Sensor Assisted Movement Identification and Prediction for Beamformed 60 GHz Links. In *Proc. of IEEE CCNC* (2015).
[5] Ghasempour, Y., da Silva, C. R., Cordeiro, C., and Knightly, E. W. IEEE 802.11 ay: Next-Generation 60 GHz Communication for 100 Gb/s Wi-Fi. *IEEE Communications Magazine 55*, 12 (2017), 186–192.
[6] Ghasempour, Y., Prasad, N., Khojastepour, M., and Rangarajan, S. Link Packing in mmWave Networks. In *Proc. of IEEE ICC* (2017).
[7] Haider, M. K., and Knightly, E. W. Mobility Resilience and Overhead Constrained Adaptation in Directional 60 GHz WLANs: Protocol Design and System Implementation. In *Proc. of ACM MobiHoc* (2016).
[8] IEEE. 802.11ay task group. http://www.ieee802.org/11/Reports/tgay_update.htm.
[9] Lee, S., and Jung, S.-Y. Location Awareness using AoA based Circular-PD-Array for Visible Light Communication. In *Proc. of APCC* (2012).
[10] Ma, J., Weidenbach, M., Guo, R., Koch, M., and Mittleman, D. Communications with THz Waves: Switching Data Between Two Waveguides. *Journal of Infrared, Millimeter, and Terahertz Waves 38*, 11 (2017), 1316–1320.
[11] Nitsche, T., Cordeiro, C., Flores, A., Knightly, E., Perahia, E., and Widmer, J. IEEE 802.11ad: Directional 60 GHz Communication for Multi-Gigabit-per-second Wi-Fi. *IEEE Communications Magazine 52*, 12 (2014), 132–141.
[12] Nitsche, T., Flores, A. B., Knightly, E. W., and Widmer, J. Steering with Eyes Closed: mm-Wave Beam Steering without In-Band Measurement. In *Proc. of IEEE INFOCOM* (2015).
[13] Ravindranath, L., Newport, C., Balakrishnan, H., and Madden, S. Improving Wireless Network Performance using Sensor Hints. In *Proc. of USENIX NSDI* (2011).
[14] Saha, S. K., and et.al. X60: A Programmable Testbed for Wideband 60 GHz WLANs with Phased Arrays. In *Proc. of ACM WinTech* (2017).
[15] Singh, S., Ziliotto, F., Madhow, U., Belding, E. M., and Rodwell, M. Blockage and Directivity in 60 GHz Wireless Personal Area Networks. *IEEE JSAC 27*, 8 (2009), 1400–1413.
[16] Sur, S., Pefkianakis, I., Zhang, X., and Kim, K.-H. WiFi-Assisted 60 GHz Wireless Networks. In *Proc. of ACM MobiCom* (2017).
[17] Sur, S., Venkateswaran, V., Zhang, X., and Ramanathan, P. 60 GHz Indoor Networking through Flexible Beams: A Link-Level Profiling. In *Proc. of ACM SIGMETRICS* (2015).
[18] Sur, S., Zhang, X., Ramanathan, P., and Chandra, R. BeamSpy:Enabling Robust 60 GHz Links Under Blockage. In *Proc. of NSDI* (2016).
[19] TP-Link. Talon ad7200 multi-band router. http://www.tp-link.com/en/products/details/AD7200.html.
[20] Wei, T., Zhou, A., and Zhang, X. Facilitating Robust 60 GHz Network Deployment By Sensing Ambient Reflectors. In *Proc. of USENIX NSDI* (2017).
[21] Xiong, J., and Jamieson, K. ArrayTrack: A Fine-Grained Indoor Location System. In *Proc. of USENIX NSDI* (2013).
[22] Xu, H., Kukshya, V., and Rappaport, T. S. Spatial and Temporal Characteristics of 60-GHz Indoor Channels. *IEEE Journal on Selected Areas in Communications 20*, 3 (2002), 620–630.
[23] Yang, Z., Pathak, P. H., Zeng, Y., and Mohapatra, P. Sensor-Assisted Codebook-Based Beamforming for Mobility Management in 60 GHz WLANs. In *Proc. of IEEE MASS* (2015).
[24] Zhang, C., and Zhang, X. Pulsar: Towards Ubiquitous Visible Light Localization. In *Proc. of ACM MobiCom* (2017).
[25] Zhou, A., Zhang, X., and Ma, H. Beam-forecast: Facilitating Mobile 60 GHz Networks via Model-Driven Beam Steering. In *Proc. of IEEE INFOCOM* (2017).